SEISMIC PERFORMANCE ASSESSMENT OF REINFORCED CONCRETE STRUCTURES WITH MASONRY INFILLED PANELS: THE CASE OF BLOCK # 22 OF THE SANTA MARIA HOSPITAL IN LISBON

J. Proença, Carlos S. Oliveira and J.P. Almeida
ICIST/IST, Av. Rovisco Pais, Nº 1
1049-001, Lisbon, Portugal

ABSTRACT

Early, pre-code, reinforced concrete structures present undetermined resistance to earthquakes. This situation is particularly unacceptable in the case of essential facilities, such as healthcare structures. Amongst these, the Santa Maria Hospital – finished in 1953 with a total area of 120,000 m^2 – in Lisbon, was designed without explicit consideration for earthquake loading. Given the crucial importance of this healthcare facility in the case of a strong earthquake in the greater Lisbon metropolitan area, the Portuguese Health Ministry requested a seismic vulnerability assessment of the Hospital structure, as well as of the major non-structural components, medical equipment and basic infrastructure lifelines.

The structural seismic vulnerability assessment stages comprised the development of linear dynamic and nonlinear static numerical models for some of the more representative building blocks. Nonlinear static analyses were conducted on one of the Hospital's most representative buildings according to displacement-based seismic design methodologies, as recommended by FEMA-273 (BSSC, 1997) and ATC-40 (ATC, 1996). A first nonlinear model was significantly modified through the introduction of diagonal struts, representing the stiffening effect of infill masonry walls, to match the experimentally determined fundamental frequencies. The analysis was carried out by means of two distinct nonlinear models, in terms of the load patterns. The first model (as described above) was used until all struts at a given intermediate storey collapsed, leading to a substantial change in the deformation and load pattern. The subsequent second model differed from the first model by the removal of the struts that had collapsed. A sensitivity analysis was carried out by changing the strength parameters of the diagonal struts. The final capacity curve was computed combining the former two capacity curves, and the performance point was subsequently estimated through the Capacity Spectrum Method (CSM). The results show that the structure does not collapse but the high damage concentration in the intermediate storey renders the building partially inoperative.

KEYWORDS: Performance-Based Design, Seismic Assessment, Masonry Infilled Structures, Healthcare Structures, Modal Identification

INTRODUCTION

In September 2002, DGIES – Direcção Geral de Instalações e Equipamentos de Saúde, from the Portuguese Health Ministry, requested for the seismic vulnerability assessment of one of the Portuguese largest healthcare facilities – the Santa Maria Hospital. The former study was provisionally finished in April 2003 (Oliveira et al., 2003). The Santa Maria Hospital has a total area of 120,000 m^2, presently with 1560 internment beds. The hospital complex is located in Lisbon, in the Portuguese highest seismic risk zone, with a PGA value of 0.275g for a return period of 3000 years. Recent earthquake hazard studies (Oliveira et al., 1999) pointed out that this PGA value corresponds to a return period of 975 years.

The Santa Maria Hospital building (Figure 1) consists of 47 cast-in-situ reinforced concrete frame building blocks, 1 to 11 storeys high, separated by expansion joints. The building design and construction started in the late 1930s and ended in 1953, before earthquake-resistant design clauses were included in the Portuguese structural design codes. Nevertheless, the structural designer was aware of the "earthquake peril", but considered that the RC frame structure had an intrinsic lateral force resisting strength that would suffice in the event of an earthquake.

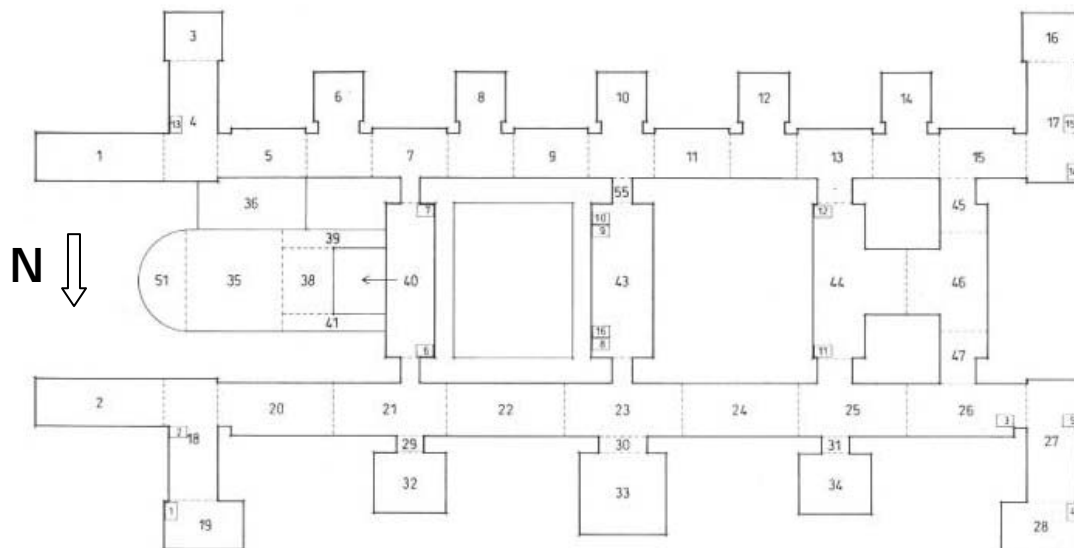Fig. 1 Aerial view of the Santa Maria Hospital campus

Fig. 2 Santa Maria Hospital: General plan and building blocks identification

PRELIMINARY ANALYSIS OF THE SANTA MARIA HOSPITAL

1. General Structural Solution

1. The Santa Maria Hospital presents two main, E-W oriented wings, with three N-S direction connection building blocks as shown in Figure 2.
2. The majority of the building blocks are 10-storeys high, whereas the corner blocks (3-4, 16-17, 18-91 and 27-28) have an extra storey, and each of these pairs of corner blocks has a 150 m³ reinforced concrete water tank on the roof.
3. The prevailing structural solution consists of cast-in-situ 2D RC frames with cast-in-situ ribbed slabs (the ribs being set perpendicular to the frame beams).
4. The building blocks were originally designed for intense wind pressures on the exposed facades, leading to the RC frames being predominantly set perpendicular to these facades. The building blocks in the two main wings have their frames in the N-S direction, with the exception of the corner blocks that present frames in both horizontal directions. The N-S direction connection blocks have their frames in the E-W direction.

5. In spite of not having been considered as a part of the (lateral or vertical) structural load-resisting system, the building blocks have structurally non-negligible internal and external masonry walls. These masonry walls contain rubble stone blocks in the lower storeys and dense ceramic bricks in the upper storeys.

6. The reinforced concrete elements' detailing is characterized by low ductility, as can be expected by: the use of smooth reinforcing bars; indicated large stirrup spacing in the columns; and outdated detailing rules (90º bends, probably insufficient anchorage lengths, etc.).

2. Relevant Design Data

1. The original structural design was carried out in accordance with the working stress design methodology.

2. The building blocks were designed for a uniformly distributed 1.47 kN/m^2 wind pressure on the exposed facades.

3. The consulted design documentation had no reference to material strengths, either steel or concrete. Inverse design calculations point to the smooth steel rebars being of class S400 (characteristic yield stress of 400 MPa or 58015 psi). The lack of information regarding the most relevant mechanical properties of both steel and concrete led to an experimental material characterization program. The average concrete compressive strength, as determined from a group of drilled concrete-core samples, was 20 MPa (2900 psi) for beam and column elements. The steel rebars yielding stress varied, depending on the bar diameters, from 299 to 358 MPa, with an average value of 307 MPa (44527 psi).
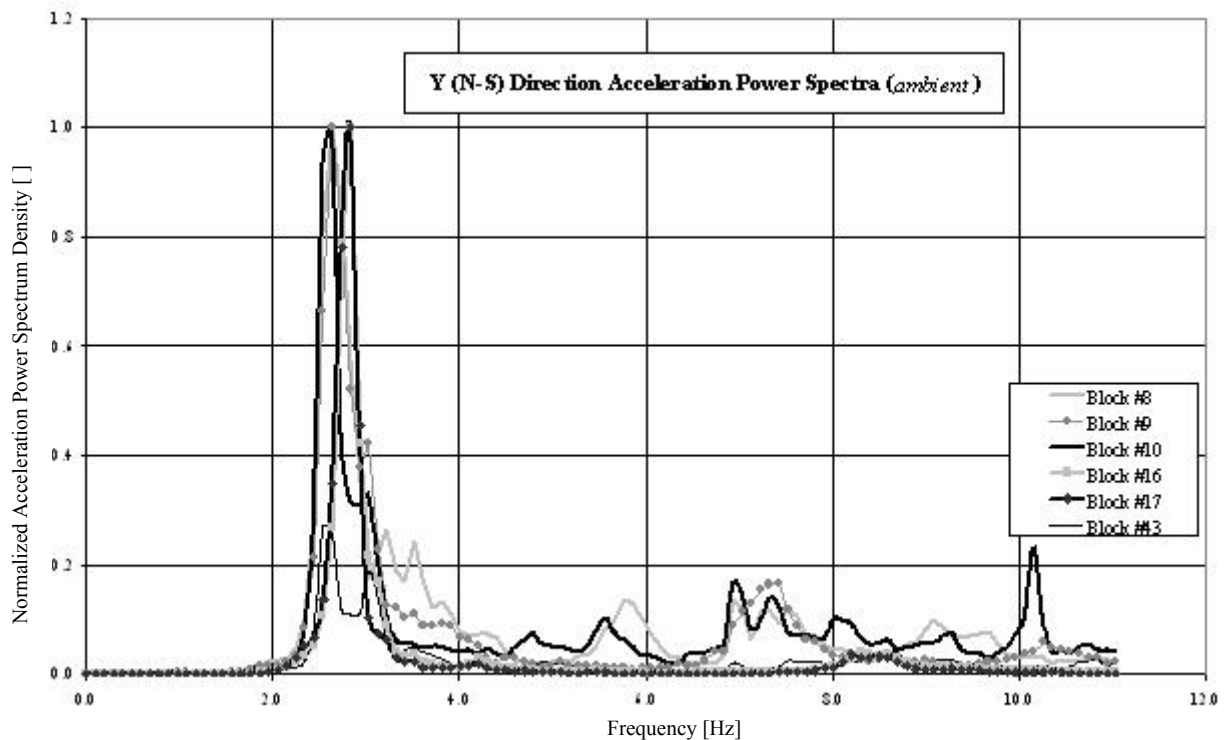

Fig. 3 Normalized ambient vibration acceleration power spectrum for building blocks # 8, 9, 10, 16, 17 and 43 (Y- or N-S direction)

3. Modal Identification

1. The lateral load structural behaviour of the building blocks is highly dependent on the effectiveness of the separation joints, as well as on the stiffness and strength contribution of the masonry wall panels. Considering these uncertainties and prior to the development of refined numerical models, a modal identification stage was carried out. The modal identification stage was subdivided into the

simplified[1] modal identification of fourteen different building blocks, amongst which was the building block # 22, and the complete[2] modal identification of building block # 4 (one of the corner building blocks).

2. The "simplified" modal identification is based on the assumption that ambient vibration excitation can be considered equivalent to a white-noise process, in which the peaks of the response power spectral density (or of its Fourier transform) correspond to the modal frequencies. Figure 3 depicts the normalized Y-direction (i.e., N-S direction) acceleration power spectra for ambient vibration records collected in building blocks # 8, 9, 10, 16, 17 and 43.

3. These results (and others not shown) clearly point out to a unified behaviour of the building blocks with a fundamental frequency value of 2.4-2.8 Hz for X- (i.e., E-W) direction and 2.4-2.8 Hz for Y- (i.e., N-S) direction.

4. The complete modal identification of building block # 4 (Ferreira, 2001) was performed according to the BFD – Basic Frequency Domain – algorithm (Ventura, 2000), leading to the mode shapes depicted in Figure 4.

5. One of the most striking results is that the maximum interstorey drift in the Y- (i.e., N-S) direction occurs within intermediate storeys, more specifically between the 3rd and 7th storeys, attaining its maximum in the 3rd storey. This fact leads to higher demands on the (RC and masonry) elements that are placed in-between these storeys.
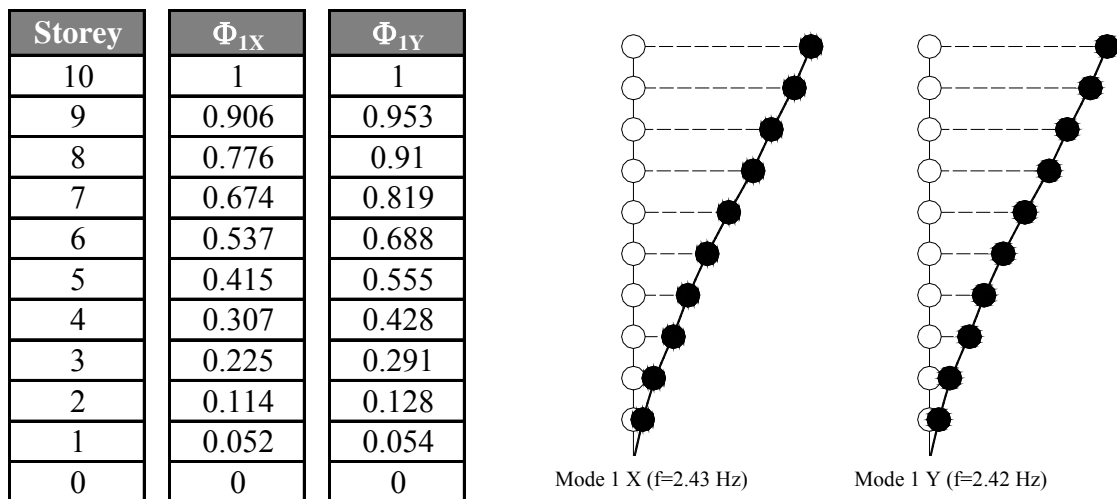
Storey	Φ_{1X}	Φ_{1Y}
10	1	1
9	0.906	0.953
8	0.776	0.91
7	0.674	0.819
6	0.537	0.688
5	0.415	0.555
4	0.307	0.428
3	0.225	0.291
2	0.114	0.128
1	0.052	0.054
0	0	0

Mode 1 X (f=2.43 Hz)   Mode 1 Y (f=2.42 Hz)

Fig. 4   Fundamental mode shapes for building block # 4 (X- or E-W direction, Y- or N-S direction)

BLOCK # 22 NUMERICAL MODELS

1. Initial Linear Model

The building block # 22 is located in the north wing of the Hospital, as shown in Figure 2. The structure consists of nine storeys, with six N-S, reinforced concrete plane frames with a spacing of approximately 5.75 m. The building plan is rectangular, 28.91×12.65 m for the first 5 floors, with a setback of 4.31 m in the direction of the frames for the top storey. The storey height varies between 3.0 and 4.0 m. The cross-sectional dimensions of members vary along the height, particularly the columns

---

[1] The "simplified" modal identification is aimed only at the identification of the fundamental frequencies, which can be accomplished by the collection of ambient vibration records at a single storey, generally the highest one.
[2] The "complete" modal identification is aimed at the identification of modal frequencies <u>and</u> modal shapes of a given building structure, requiring intensive and lengthy instrumentation of all building storeys and the collection of synchronized ambient vibration records.

whose cross-sectional area at the top floor is less than 25% of that of the lowest storey. All the slabs are one-way, spanning between the frames (Figure 5).

The building was modelled using a 3D finite element model, with frame elements representing beams and columns. Considering that the analysis was performed in the N-S direction (direction of the expansion joints), no interaction with building blocks # 21 and # 23 was accounted for. The external and internal masonry infill panels were also modelled using a pair of diagonal frame elements for each panel, the details of which are discussed later in this section. The storey slabs were represented by equivalent beams and modelled as rigid diaphragms. The nonlinear static analysis requires the consideration of the actual force-deformation relationships for all sections which, in this case, were based on the longitudinal reinforcements of the beams and columns, taken from the original project drawings. The numerical analyses (dynamic elastic and static inelastic) were carried out with the SAP2000 Nonlinear, Version 7.42 Program (CSI, 2001).
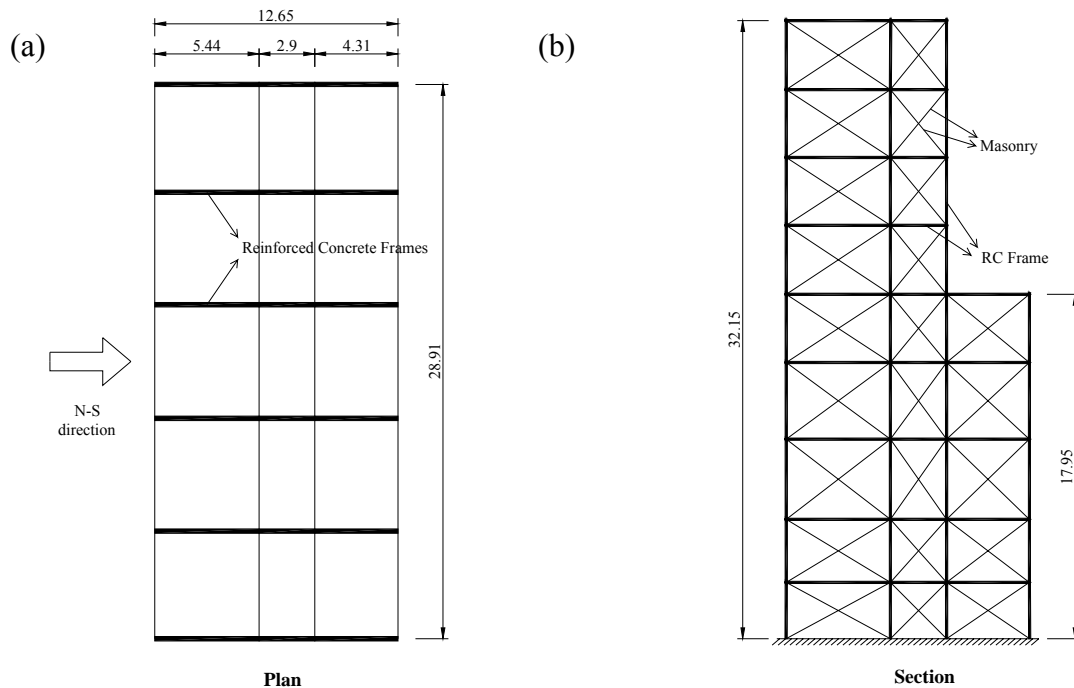

Fig. 5 Block # 22 — (a) Plan; (b) Side view

As expected, the preliminary bare RC frame numerical model led to fundamental period values much higher than the experimental ones, thus leading to the inclusion of the masonry stiffening effect in the final numerical model.

The on-site inspection led to the discrimination of two different types of masonry materials and modelling rules. In the E-W direction of the first four storeys, the masonry panels comprise rubble stone blocks (E = 5 GPa, f_w = 5 MPa, thickness = 0.5 m, where E and f_w stand for Young's modulus and crushing strength, respectively). These panels were modelled by strut elements whose widths are 15% of the diagonal length. For the remaining storeys in this direction, as well as for all the panels in the N-S direction, the solid brick blocks masonry panels (E = 3 GPa, f_w = 2.5 MPa, thickness varying from 0.20 m, in N-S direction, to 0.30 m, in average E-W direction) were modelled through diagonal struts (Fardis, 1996; Safina, 2002) with a cross-sectional area equivalent to 20% of the diagonal length of the respective panel. The cross-section shape of the struts was square (maintaining the cross-sectional area), in order to avoid the automatic reduction of member strength (computed by the program) due to slenderness effects.

The gravity loads considered in the analysis were: the dead loads for the beams, columns, slabs (with finishes) and walls (exterior and interior, based on the previously presented geometric dimensions). The dead loads due to partition walls on the slabs were 2.0 kN/m^2 and the live loads were 3.0 kN/m^2, as prescribed for hospitals in Portuguese National Codes (MHOPT, 1983). The load combination for mass calculation is: (Dead Loads) + (Live Loads)$\times \psi_2$, also based on the same standard, where ψ_2 is taken equal to 0.4. The ψ_2 coefficient takes into consideration that, when the earthquake strikes, probably only a fraction of the maximum mass will be present.

Due to the high axial stiffness of the diagonal (masonry) elements, these elements would erroneously absorb a significant fraction of the gravity loads which, in turn, would result in the reduction of the available axial strength for the subsequent lateral load increments. Taking into account the construction stages (in which the masonry is put in place after the frame construction), the former effect does not follow the actual stress distribution, since the masonry panels only carry their self-weight while the frame transfers these and other loads to the foundations. To counteract this erroneous behaviour, the diagonal strut elements were shifted out of plane, with respect to the RC frame, by a negligible amount (so as not to change the global torsional stiffness), while maintaining all the nodes of the same floor in only one diaphragm. The diaphragm as defined in SAP2000 allows for free vertical displacements at each node and, at the same time, collective horizontal motion of all in-plane nodes. One should, however, note that this method, while ensuring the transmission of the horizontal components of the strut forces to the frame elements, does not allow for the transmission of the vertical components. Additional analyses, not included in the present paper, show that the bending and shear forces in the surrounding frame elements are not significantly affected by this modelling assumption. However, the same analyses show that there are substantial differences in terms of the axial forces in the frame elements as well as in the masonry struts.

After the inclusion of the masonry infill stiffening effect, the numerical model yielded fundamental frequency values in close agreement with the experimentally determined ones as shown in Table 1.

Besides the introduction of diagonal elements to model the masonry, some modification factors were also applied to the flexural stiffness of the RC elements, as recommended in Table 9-3 of ATC-40 (ATC, 1996).

Table 1: Comparison between Experimental and Analytical Frequencies

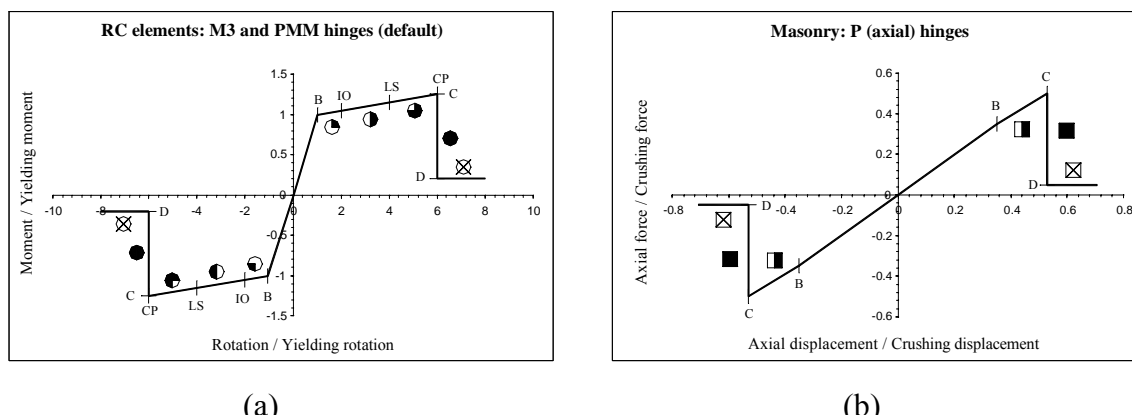|	Experimental		Analytical	
	Direction	Frequency [Hz]	Direction	Frequency [Hz]
1st Mode	N-S	2.42	N-S	2.05
2nd Mode	E-W	2.43	E-W	2.63
3rd Mode	Torsional	3.80	Torsional	4.29

Fig. 6 (a) Concrete hinges (damage symbols); (b) Masonry hinges (damage symbols)

2. Nonlinear Model and Actions

The structural model referred to so far was further refined in order to perform a nonlinear static (pushover) analysis. The Capacity Spectrum Method (CSM), as proposed by ATC-40 (ATC, 1996), was followed. The CSM allows for the consideration of the complex, but representative, behaviour of the structure and has a clearer physical support than other, equally disseminated, nonlinear static procedures (the Displacement Coefficient Method, DCM, and the N2 Method). Besides, CSM has been recommended (Albanesi et al., 2002) as a method that, when compared with nonlinear dynamic analyses, satisfactorily predicts maximum displacements for all structural types, including tall frame structures.

A pushover analysis model requires a series of hinges to account for the nonlinear behaviour of the various structural elements which, in this case, are the RC beams and columns and the masonry elements. SAP2000 generates the hinges for the beam and column elements based on the modelled reinforcement, the material characteristics, and on the provisions of both ATC-40 (ATC, 1996) and FEMA-273 (BSSC, 1997) (see Figure 6(a)). The nonlinear structural model comprised PMM hinges (P – axial force; MM – bi-axial moments) for columns, M3 hinges (uniaxial moment) for beams, and P hinges (axial force) for the diagonal strut elements. The inferior bond of the smooth reinforcing bars was implicitly considered in the algorithm used to determine the performance point, but was not explicitly accounted for in the modelling stages. This inferior bond may lead to a reduction in the anticipated strength, as well as in the plastic hinge length and in the available rotational ductility. Each beam was discretized into two finite elements due to different reinforcement detailing near each column joint.

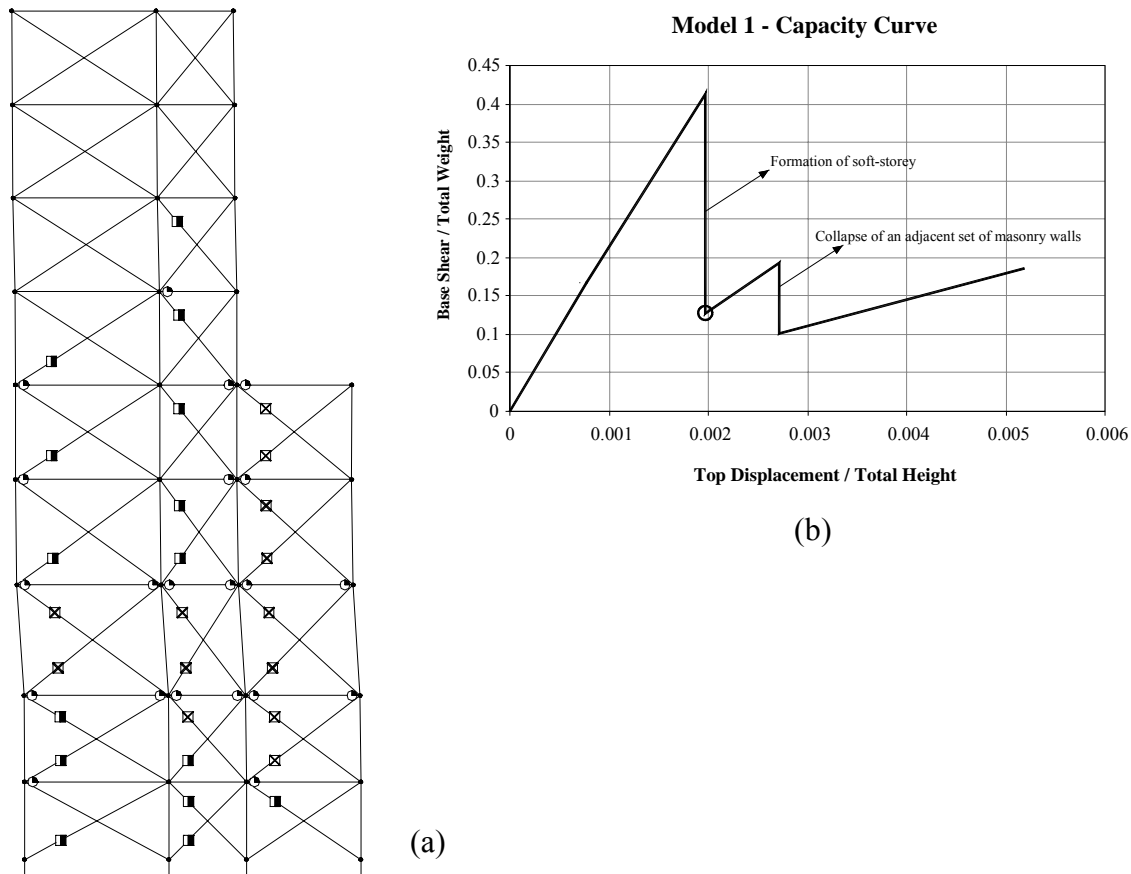(a)

Model 1 - Capacity Curve

(b)

Fig. 7   Model 1 — (a) Layout of damage at the instant of soft-storey formation (for damage symbols refer to Figure 6); (b) Capacity curve based on first mode loading

Since the masonry tensile strength is negligible, only its compressive strength was considered. This parameter was computed by SAP2000 based on the cross-sectional area of the struts and on the allowable compressive stress. The ratio between the crushing and the cracking strengths was taken as 1.44 (Pires, 1990). Moreover, the crushing to cracking displacement ratio was taken as 1.5. Finally, to prevent numerical instabilities, this hinge was modified as shown in Figure 6(b), in such a way that the total compressive strength is equally divided into compressive and tensile zones. The modelling of the masonry infill could alternatively have been done by means of a single compressive strut. This alternative model would be closer to reality since the masonry panel has a limited capacity of withstanding tensile forces. However, both of these methods neglect the localized effects on the beam and column elements induced by the finite width of the masonry struts that could lead to premature shear failure in columns in the hinge zone.

The model did not explicitly consider the possibility of shear failure in the columns, which was verified 'a posteriori'. Beam-column joints were assumed to keep their integrity during the analysis stages.

Another important aspect in pushover analyses is the definition of the lateral loads which, in this case, were considered proportional to the product of the storey masses and the fundamental elastic mode shape, assuming that this mode accurately describes the predominant response pattern of the structure. This approach is classified as 'Level 3' (ATC, 1996) and is recommended by the Applied Technology Council for buildings with fundamental mode periods up to about one second, such as the one under study.

The pushover analysis was carried out in two sequential stages: a first stage involving the application of the gravity loads; and a second stage in which the lateral loads were incrementally applied.

The seismic action was defined by the 5% damping response spectrum (CEN, 2003), calibrated for the seismic zone of Lisbon. This response spectrum was further converted and fitted to the parameterized response spectrum that CSM methodology considers. The best fit values for the seismic coefficients were: $C_a = 0.275g$ and $C_v = 4.05$ m/s. The final response spectrum was represented in the Acceleration-Displacement Response Spectrum (ADRS) format.
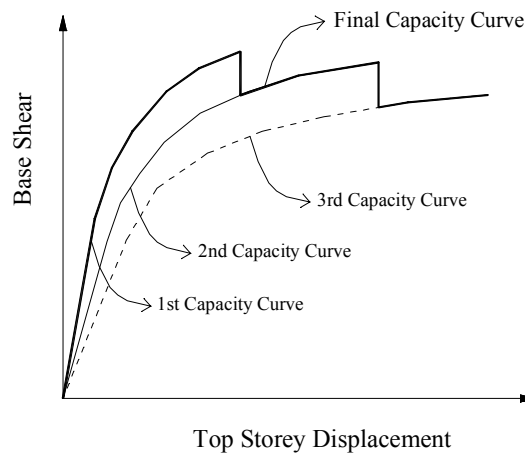

Fig. 8 ATC pushover curve, obtained from several capacity curves, as indicated in ATC (1996)

PUSHOVER ANALYSIS

In the E-W direction the behaviour of building block # 22 is dependent on the behaviour of the remaining blocks along the North wing, making the individual analysis along this direction of the building block clearly unrealistic. Consequently, the pushover analysis was performed solely in the N-S direction, coincidental with the direction of the main frames. The expansion joints are, therefore, stressed along the tangential axis, enhancing the likelihood of the individual behaviour of the building block # 22.

The application of the gravity loads was performed in one single step due to the fact that none of the elements reached its yield or cracking strength.

As referred previously, the lateral load pattern applied along the building height was based on the elastic fundamental mode. The increments of this lateral load pattern led to the capacity curve presented in Figure 7(b) in terms of the normalised base shear versus drift. This curve shows the yielding, cracking and crushing sequence of the various elements — as expected, the masonry elements are the first to crack – the top three storeys are the least affected, while the lower ones present generalized degradation. For increasing top displacement values, damage tends to concentrate at the intermediate levels (2nd, 3rd and 4th storeys), and, for a drift value of 0.00198, all struts at the 3rd storey reach their ultimate strength. Further, loading increments result in the development of the well-known soft-storey phenomenon. Figure 7(a) shows the damage inflicted, both in the masonry and in the reinforced concrete elements, at this step, even though, as previously described, these two structural elements are considered to exist in different parallel planes. More masonry elements at other levels have also reached their ultimate capacity at the onset of the soft-storey mechanism. The damage in the RC elements is limited to yielding in some beams, especially those at the second and third levels.

At certain stage in the lateral loading increments, it is likely that an element (or group of elements) starts to significantly lose its (their) strength. In such cases, new capacity curves have to be generated in

order to model the overall loss of strength. It is convenient to reduce or eliminate the stiffness of the damaged element (or group of elements) and create the additional capacity curves to an accurate global structural characterization – the final composite curve is assembled from these different capacity curves. The transition from one capacity curve to the following is done at the displacement corresponding to the strength degradation of the first curve - the final pushover curve resembles a saw tooth shape, as shown in the generic curve of Figure 8, proposed by ATC-40 (ATC, 1996).

To compute the demand, the CSM methodology makes use of a series of trial performance points, for which damping estimation is based on a bilinear representation of the capacity spectrum. In the case of a saw tooth capacity spectrum this bilinear representation should be based on the capacity spectrum curve that describes the behaviour at the tested displacement. Consequently, only elements that influence the mass or the stiffness of the structure at (or near) the performance point are of interest for the analytical model.

Stiff and weak masonry panels, used in most contemporary building structures, would eventually degrade their stiffness and strength long before reaching the structural performance point. Based on this assumption, the common practice in structural assessment of RC structures disregards the contribution of these infill panels. However, as most other structures of the same construction period, the Santa Maria Hospital building blocks include some relatively strong material masonry infill that should not be overlooked, since its damage and subsequent failure can drastically modify the behaviour of the lateral force resisting system. The CSM methodology was applied to the case under study with some adaptations to the standard procedure as explained afterwards.

The formation of the soft storey is the first noteworthy drop in the lateral load system strength (marked with $\bigcirc$ in the capacity curve of Figure 7(b)) – the structure remains very stiff until the collapse of the intermediate storey infilled masonry set of walls. As stated, the analysis led to the formation of a weak 3rd storey, yet sensitivity analyses carried out afterwards showed that the soft-storey phenomenon can take place either in the 2nd or in the 4th levels, depending on the strength parameters of the diagonal struts. The critical role of the infill masonry walls leads to a sudden lateral strength degradation of over 65%. Crushing of these struts leads to a major transformation in the first mode shape and, consequently, also in the lateral load pattern that should be applied to the structure to evaluate its performance. Hence, this model is no longer valid for the subsequent structural assessment stages and a new model, therefore, had to be developed.

The formation of a weak 3rd storey can be explained by the combination of the following two main causes: the total storey shear at the 3rd storey is only slightly inferior (−3.8%) to the base shear (as a consequence of the applied force pattern being proportional to the fundamental mode shape); and the total column cross-sectional area at the 3rd storey is 65% of that at the base, leading to a relative increase in the strut stresses at the referred level. The collapse of the remaining struts at the 2nd, 4th and 5th storeys is a direct consequence of the geometrical irregularity induced by the setback.

In the 2nd, damaged model, all the elements that have attained their ultimate capacity (i.e., the diagonal masonry struts represented by $\boxtimes$ in Figure 7(a)) at the instant of the soft-storey formation are removed, as can be seen in Figure 9(a).

According to ATC-40 (ATC, 1996) and as previously clarified and generically shown in Figure 8, the final capacity curve is determined combining the different capacity curves at the displacement corresponding to each strength degradation, which is realistic provided that there is a limited strength degradation. For the actual building and soft-storey phenomenon this assumption turns out to be unacceptable – the reasons for this statement are explained later in this paper.

An alternative to accurately progress with the analysis would consist in the change of model 2 in order to make it valid since the beginning of the application of the new lateral loads. Besides the aforementioned elimination of the collapsed elements, this change would require the stiffness reduction for all the degraded elements, as well as the reproduction of the exact deformation and stress state of each element. However, commercially available programmes (as the one used) are still not capable of automatically performing the preceding steps and, moreover, the manual introduction of all these changes is practically impossible. Hence it was decided to use a simplified (although coarse) process to take into account the expected building performance. The chosen adapted methodology is based on a rational interpretation of how the several (in this case, only two) capacity curves can be combined to obtain more precise results.
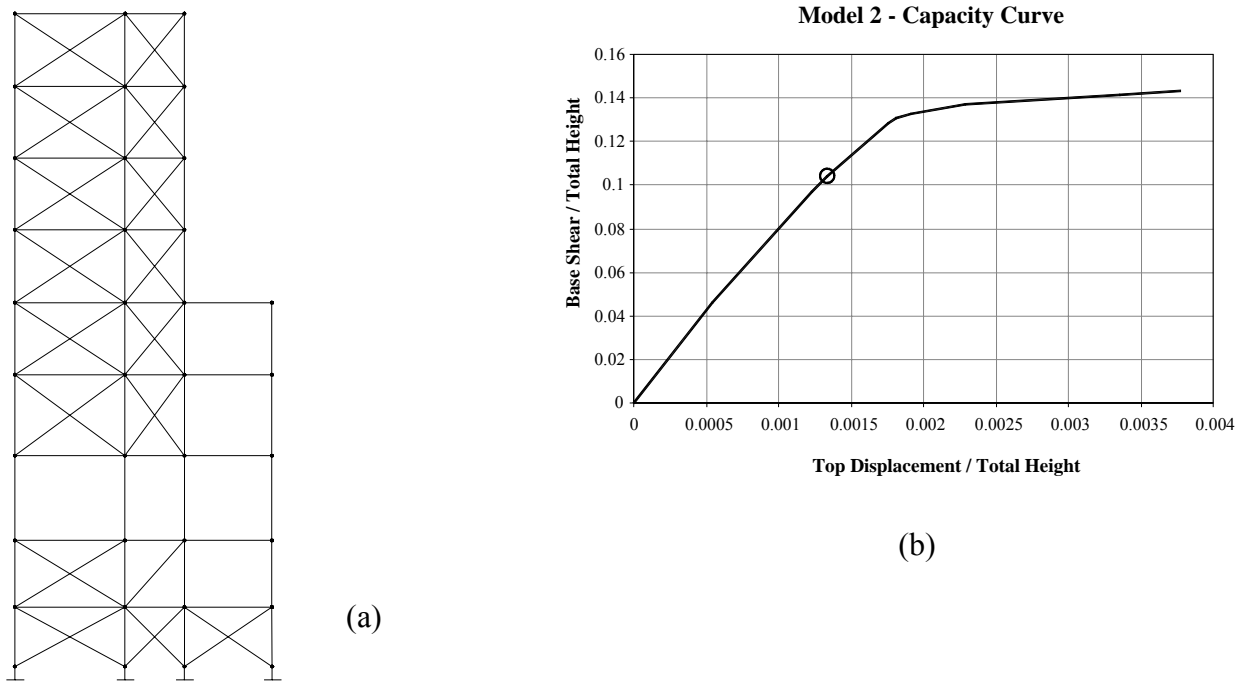
(a)

Model 2 - Capacity Curve

(b)

Fig. 9 Model 2 — (a) Removal of collapsed masonry struts; (b) Capacity curve based on first mode (for Model 2)

(a)   (b)
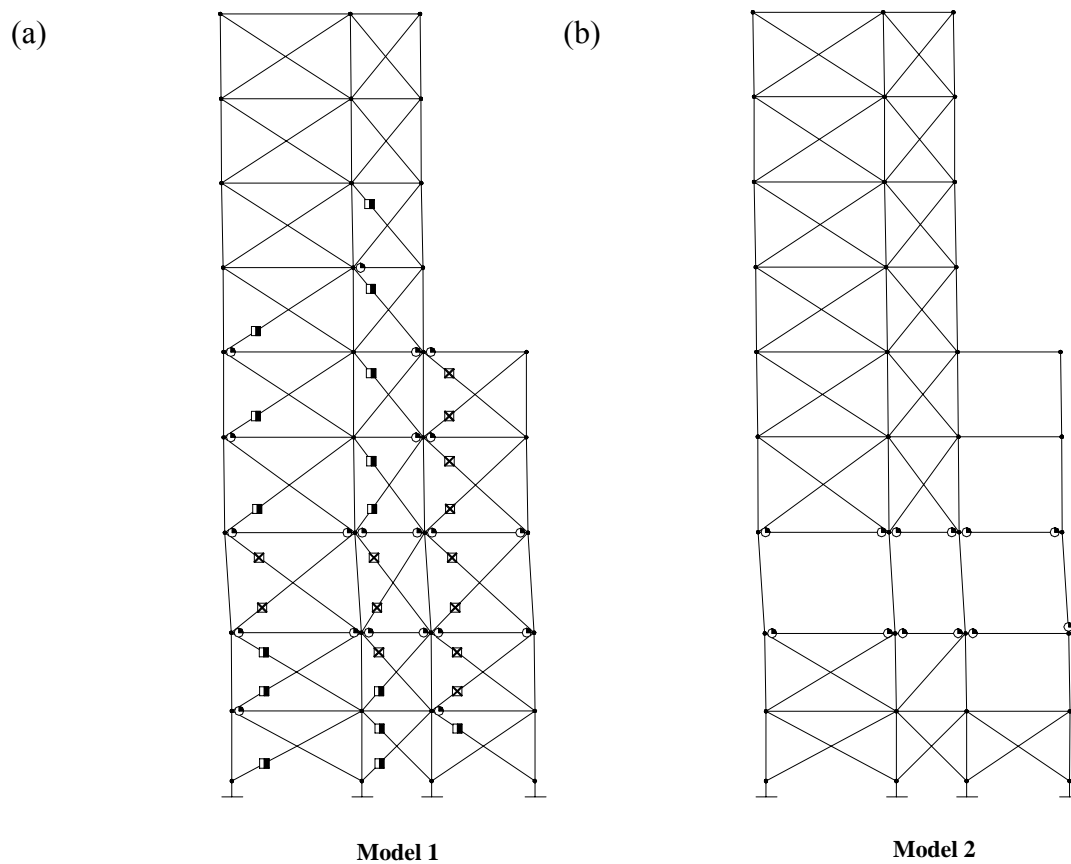
Model 1   **Model 2**

Fig. 10 Comparison of the "equivalent" stage between Model 1 and Model 2 (for damage symbols refer to Figure 6)

After running the pushover analysis with Model 2 (whose capacity curve is shown in Figure 9(b)), the first step consisted in the observation of the deformation distribution and progression throughout the elements. The high lateral forces applied at the soft storey level have led to large demands of deformation capacity in the column and beam elements in that vicinity. In contrast, all remaining RC elements are kept practically undeformed, without significant stresses, even for considerable drift values of 0.003 (top displacement of 0.10 m). The only masonry elements that were subjected to significant axial force increments are placed above and below the soft-storey, however never reaching, the cracking strength for the same extreme top displacement values.

The point in the capacity curve of Model 2 from which the structural system would continue to be represented was determined comparing the degradation of the reinforced concrete frames of Model 1 (at the onset of the soft-storey mechanism) with the progressive degradation of the same components of Model 2. In fact, there is a value of the base shear (marked with ○ in the 2nd capacity curve of Figure 9(b)) for which the deformation of the RC elements adjacent to the soft storey is reasonably similar to that of Model 1 at the onset of soft storey mechanism (see comparison in Figure 10). This is the stage beyond which the final capacity curve of the structure should follow the capacity curve of Model 2. It is clear that there are a significant number of differences between these two stages, making these two not totally "compatible". Nevertheless, damage in the RC elements neighbouring the 3rd storey was considered, by far, the most important similarity to account for with care. In fact, the deformation of the RC concrete elements outside the 3rd storey is not crucial, since these are not subjected to subsequent high demands – i.e., the lateral displacement, after the soft-storey, is mainly due to the deformation of the columns and beams of this level. For the masonry, the most notorious discrepancy between the two compared stages is the several panels that had achieved the cracking strength in Model 1 but were modelled with the initial stiffness in Model 2. This inconsistency can be, however, disregarded because the assumed post-cracking stiffness is almost identical to the initial one (see Figure 6(b)). The key task left is to precisely find out whether the stress increment in the masonry elements of the level above and below the soft-storey is enough to cause their collapse (and consequently, lead to new soft-storey formation) before the performance point is attained.
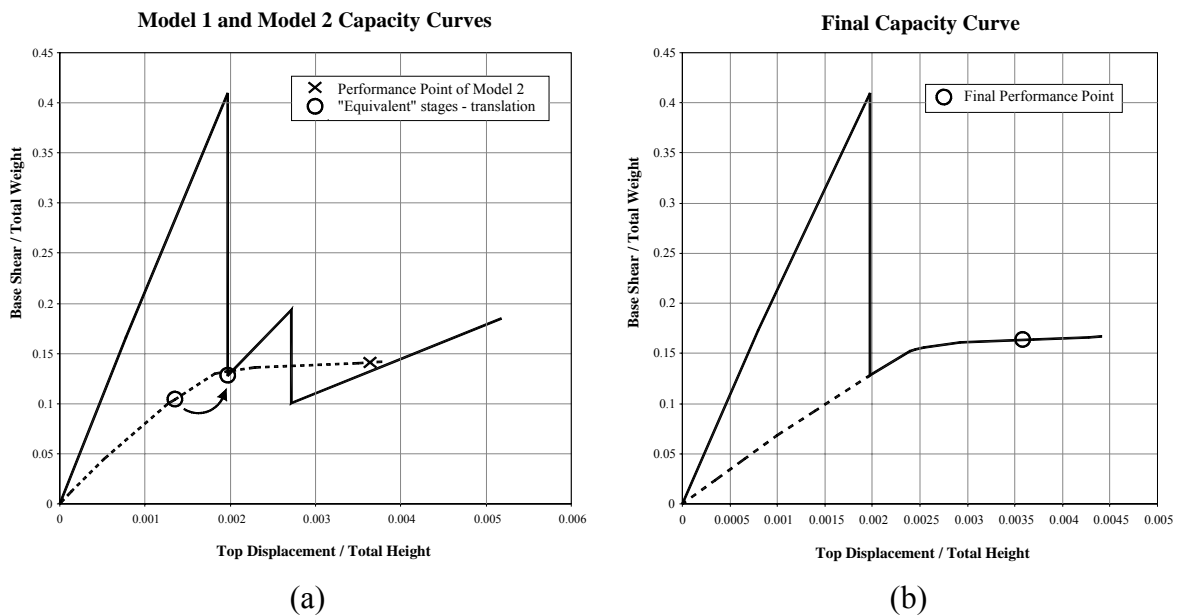

Fig. 11 (a) Capacity curve for each model; (b) Final capacity curve

The final capacity curve is obtained by combining the first part of the capacity curve of Model 1 with the second part of the capacity curve of Model 2 (Figure 11(a)). The result can be observed in Figure 11(b).

Using all this information, it is now possible to determine the demand for which the steps indicated in 'Procedure A' of ATC-40 (ATC, 1996) are followed. The conversion of the capacity curve to the capacity spectrum is depicted in Figure 12(a). The remaining steps of the procedure were implemented in a

graphical/numerical computer program, specifically created for this task (see Figure 12(b)). This program has the following particular features:

- the first trial performance point is obtained by using the equal displacement approximation;

- the Hospital has been classified as a 'Poor Existing Building', due to the fact that ductility is not assured (large stirrup spacing, smooth rebars, and outdated, non-ductile detailing);

- the spectral reduction factors were computed in accordance with the equations proposed by Newmark and Hall (Newmark and Hall, 1982).
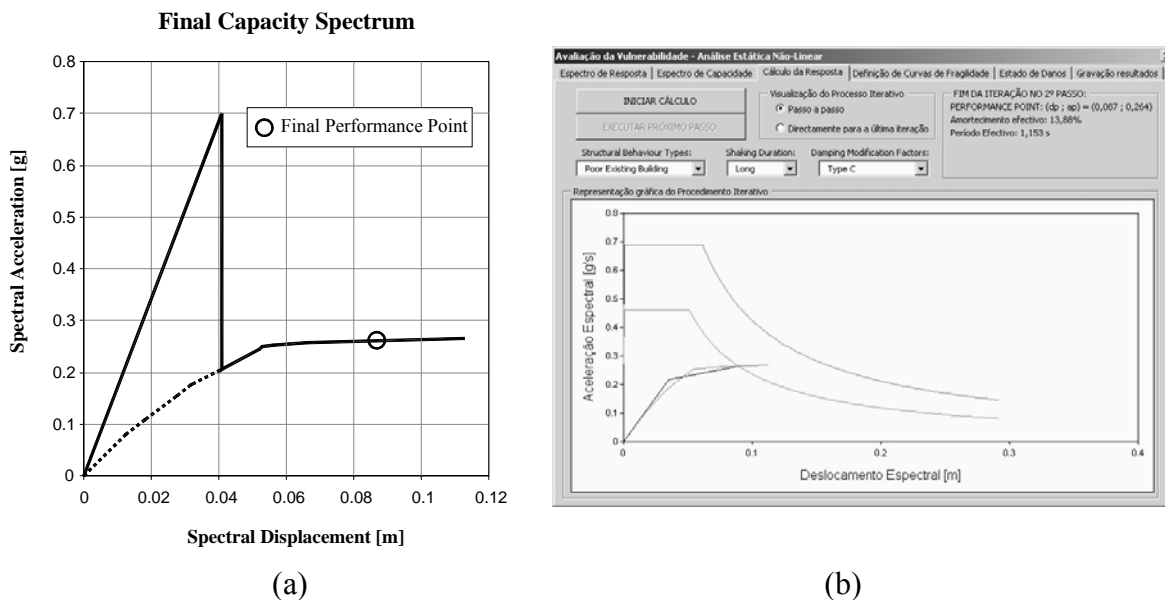

Fig. 12 (a) Capacity spectrum; (b) Performance point determination

The performance point (PP) result of this method is, in spectral coordinates, (0.264g, 0.087 m) which, in terms of normalised base shear versus drift represents a demand of (0.1638, 0.0036). The corresponding base shear and top displacement values are, respectively, 7979.98 kN (1726.5 kips) and 0.1153 m (4.53 in). The final base shear is composed of 6007.08 kN of Model 1 and only 1672.9 kN of Model 2. It should be noted that the equivalent viscous damping is 13.88%, for a period that is lengthened from an initial value of 0.488 s to 1.153 s.

After the determination of PP, it is possible to make the reverse conversion and identify the top displacement of Model 2 that corresponds to PP. A detailed analysis of the stress increment and deformation development in the masonry elements of Model 2 was carried out for the loading stages in Model 2 capacity curve. The main conclusion is that the observed stress increments in the truss elements, when added to the stress levels resulting from Model 1, will not lead to the formation of another soft storey. Plastic hinge formation at PP can be observed in Figure 13(a), which was assembled from results of Model 1 (for concrete elements outside the soft-storey and masonry) and Model 2 (for concrete elements adjacent to the soft-storey).

As can be seen from Figure 13(a), although the risk of life-threatening injury is not negligible, some margin against total or partial structural collapse remains. Figure 13(b) shows the storey shear distribution for the calculated demand.

If the CSM was literally applied to the structure (i.e., by using the capacity spectrum obtained for the second model), the estimated PP would be (0.1426, 0.0036), in terms of normalised base shear versus drift. These values generally seem in agreement with those obtained by the preceding procedure. However, if the previous damage pattern at performance point (Figure 13(a)) is compared to that obtained for Model 2 (Figure 14), it is clear that there are some features of the structural performance that cannot be correctly predicted by this latter model alone: the damage in elements outside the soft-storey (either RC or infill panels) is largely underestimated, while the deformation in RC elements of the 3rd storey is overestimated.

The available design drawings included scarce information as to the stirrup spacing and detailing, thus hampering the final verification of the shear failure of the columns. However, considering the stirrup detailing and spacing as shown in these drawings, 'a posteriori' computations showed that in some of the columns of the 3rd storey the available strength was inferior to the shear force values at the performance point. This fact, if confirmed, implies that shear failure of these columns would have occurred before the attainment of the former point.
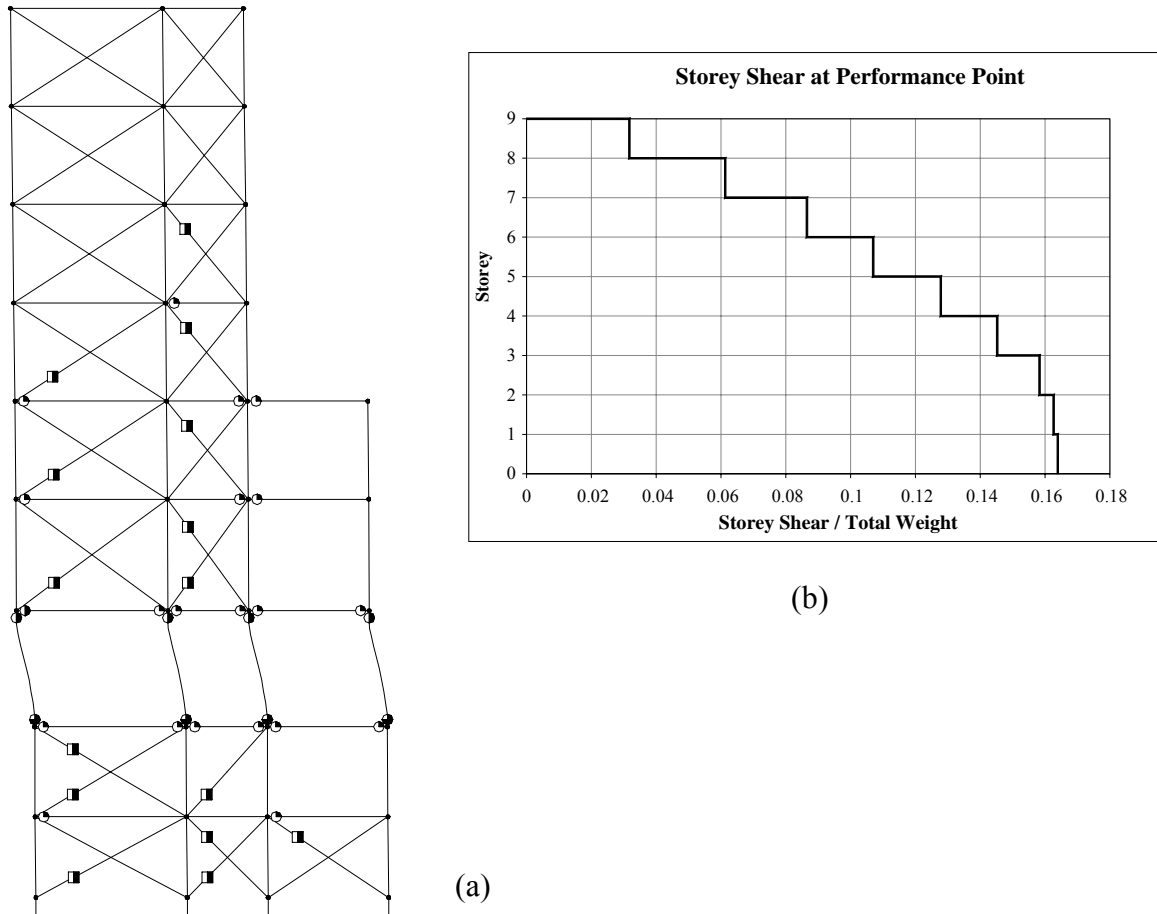
Fig. 13 (a) Expected damage description for concrete and masonry at performance point; (b) Storey shear (for damage symbols refer to Figure 6)

Considerable engineering judgement has to be employed before linking base shear versus roof displacement curves "vertically", as presented in ATC-40 (ATC, 1996). In fact, for small strength losses, the determination of the performance point can be uniquely based in the capacity curve of a single model including components influencing structural response at or near the performance point. On the other hand, high strength losses should be dealt with special care before progressing with the analysis. Sometimes, simple additional models have to be necessarily developed, as the one referred to as Model 2, for a more precise structural characterization or, at least, for the validation of the assumed hypothesis.

CONCLUSIONS

Performance-based seismic vulnerability assessment of existing structures can greatly benefit from possible modal identification stages that can show unexpected strength and stiffness contribution of secondary structural or non-structural components. In the particular case of early RC structures, strong masonry walls, either facade or partition walls, have a significant stiffening effect that greatly determines the early nonlinear stages and can, as was the case, lead to a sudden drop of strength (and stiffness). From this stage on, damage tends to concentrate in-between two particular storeys, leading to an incipient soft storey mechanism. The structural behaviour is changed to such an extent after the onset of the soft storey mechanism that a new "damaged" nonlinear model has to be developed. The successful combination of

the corresponding two capacity curves, and the subsequent performance point estimation, has to be carried out matching the damage distribution and severity at the onset of the soft storey mechanism. One should, however, stress that the implementation of displacement-based methodology with widely disseminated FEM programs, has to be complemented with sound engineering judgement, notably in the combination of different and succeeding capacity spectra.

The results obtained in building block # 22 have shown that, although collapse is not imminent, there is a large possibility of extreme damage concentration between two particular storeys, leading to high localized interstorey drift demands that could undermine the Hospital's functionality.
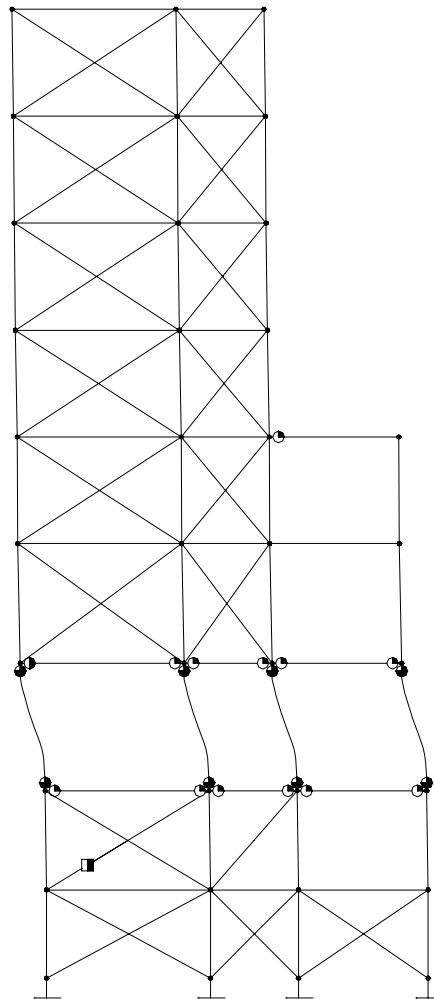

Fig. 14 Expected damage description for concrete and masonry at performance point for Model 2 (for damage symbols refer to Figure 6)

ACKNOWLEDGEMENTS

REFERENCES

1. Albanesi, T., Nuti, C. and Vanzi, I. (2002). "State of the Art of Non-linear Static Methods", Proceedings of the Twelfth European Conference on Earthquake Engineering, London, U.K., Paper 602.

2. ATC (1996). "Seismic Evaluation and Retrofit of Concrete Buildings", Report ATC-40, Applied Technology Council, Redwood City, California, U.S.A.

3. BSSC (1997). "NEHRP Guidelines for the Seismic Rehabilitation of Buildings", Report FEMA-273 (prepared by the Building Seismic Safety Council), Federal Emergency Management Agency, Washington, DC, U.S.A.

4. CEN (2003). "Eurocode 8: Design of Structures for Earthquake Resistance – Part 1: General Rules, Seismic Actions and Rules for Buildings", prEN 1998-1, Doc CEN/TC250/SC8/N335, Comité Européen de Normalisation, Brussels, Belgium.

5. CSI (2001). "SAP2000 Non-linear Version 7.42: Structural Analysis Program", Computers and Structures, Inc., Berkeley, California, U.S.A.

6. Fardis, M.N. (1996). "Experimental and Numerical Investigations on the Seismic Response of R.C. Infilled Frames and Recommendations for Code Provisions", ECOEST-PREC8 Report No. 6, Laboratório Nacional de Engenharia Civil (LNEC), Lisbon, Portugal.

7. Ferreira, P. (2001). "Identificação Modal com Vibração Ambiente – Contributo Para a Avaliação da Vulnerabilidade Sísmica do Corpo 4 do Hospital de Santa Maria", M.Sc. Thesis (in Portuguese), Instituto Superior Técnico (IST), Lisbon, Portugal.

8. Oliveira, C.S., Sousa, M.L. and Costa, A.C. (1999). "Contribuição Para a Revisão da Acção Sísmica em Portugal Continental no Contexto do Eurocódigo 8", Proceedings of the Fourth Portuguese National Meeting on Seismology and Earthquake Engineering (in Portuguese), Universidade do Algarve, Faro, Portugal, pp. 153-164.

9. Oliveira, C.S., Proença, J., Almeida, J.P. and Ferreira, P. (2003). "Programa de Avaliação da Vulnerabilidade Sísmica das Instalações Hospitalares da Área Metropolitana de Lisboa: Estudo-Piloto do Hospital de Santa Maria", ICIST-EP Report No. 25/03 (in Portuguese), Instituto de Engenharia de Estruturas, Território e Construção (ICIST), Lisbon, Portugal.

10. MHOPT (1983). "Regulamento de Segurança e Acções para Estruturas de Edifícios e Pontes" (in Portuguese), Imprensa Nacional da Casa da Moeda, Lisbon, Portugal.

11. Newmark, N.M. and Hall, W.J. (1982). "Earthquake Spectra and Design", Engineering Monographs on Earthquake Criteria, Structural Design and Strong Motion Records, Earthquake Engineering Research Institute, Berkeley, California, U.S.A., Vol. 3.

12. Pires, F. (1990). "Influência das Paredes de Alvenaria no Comportamento de Estruturas Reticuladas de Betão Armado Sujeitas a Acções Horizontais", Specialist Thesis (in Portuguese), Laboratório Nacional de Engenharia Civil (LNEC), Lisbon, Portugal.

13. Safina, S. (2002). "Vulnerabilidad Sísmica de Edificaciones Esenciales. Análisis de su Contribución Al Riesgo Sísmico", Ph.D. Thesis (in Spanish), Universidad Politécnica de Cataluña (UPC), Barcelona, Spain.

14. Ventura, C.E. (2000). "Identification by the Basic Frequency-Domain (BFD) Technique" in "Modal Identification of Output-Only Systems", Course Notes by Carlos Ventura and Rune Brincker, Universidad Politecnica de Madrid, Madrid, Spain.